Enhanced Ferroelectric and Piezoelectric Properties of (1−x)PMN-xPT Ceramics Based on a Partial Oxalate Process

Jinhwan Kim [1], Sanghyun Yoon [1], Jae-Hoon Ji [1], Young-Ho Ko [2], Kyung-Ho Cho [2], Sang-Kwon Lee [3] and Jung-Hyuk Koh [1,*]

[1]   School of Electrical and Electronics Engineering, Chung-Ang University, Seoul 06974, Korea; kjh2203kjh@naver.com (J.K.); moon_light90@naver.com (S.Y.); hoon2441@naver.com (J.-H.J.)
[2]   Agency for Defense Development, Daejeon 34186, Korea; kohjunghyuk@hanmail.net (Y.-H.K.); redskin99@naver.com (K.-H.C.)
[3]   Department of Physics, Chung-Ang University, Seoul 06974, Korea; sangkwonlee@cau.ac.kr
*   Correspondence: jhkoh@cau.ac.kr; Tel.: +82-2-820-5311

check for updates

Abstract: The pyrochlore phase in ferroelectric and piezoelectric materials is the main obstacle device application due to its poor electrical properties. Especially, the pyrochlore phase is frequently observed in the perovskite-based metal-oxide materials including piezoelectric and ferroelectric ceramics, which are based on solid-state reaction methods for fabrication. To overcome these problems, advanced innovative methods such as partial oxalate process will be investigated. In this method, crystalized magnesium niobite (MN) and lead titanate (PT) powders will be coated with a certain amount of lead oxalate and, then, the calcination process can be carried out to form the PMN-PT without pyrochlore phase. In this study, (1−x)PMN-xPT ceramics near the morphotropic phase boundary (MPB), with compositions of x = 0.25–0.40, have been prepared employing the partial oxalate method at various temperatures. The crystalline, microstructure, and piezoelectric properties of (1−x)PMN-xPT ceramics depending on the sintering temperature were intensively investigated and discussed. By optimizing the sintering temperature and compositions from the PMN-PT ceramics, the maximum value of the piezoelectric charge coefficient (d_{33}) of 665pC/N, planar electromechanical coupling factor (k_p) of 77.8%, dielectric constant (ε_r) of 3230, and remanent polarization (P_r) of 31.67 μC/cm^2 were obtained.

Keywords: piezoelectric; PMN-PT; partial oxalate process

1. Introduction

Pb(Mg$_{1/3}$Nb$_{2/3}$)O$_3$ (PMN) is a well-known relaxor ferroelectric material that has a high dielectric constant (around −10 °C) with broad diffuse and dispersive phase transition [1,2]. PbTiO$_3$ (PT) is a normal ferroelectric material, it shows piezoelectric behavior and has a Curie temperature (T_c) of 490 °C [3,4]. By employing a solid solution process, PT composition can be varied in the PMN-PT ceramics. PMN-PT can be employed in varied devices such as sensors, actuators, and transducers to substitute PZT materials because of its outstanding properties [5,6]. Especially, (1−x)PMN-xPT ceramics in the PT composition range between 0.32 and 0.35 mol, and show a morphotropic phase boundary (MPB) between the rhombohedral and tetragonal phases [7–9]; it also shows high piezoelectric and ferroelectric properties. However, the formation of a lead niobate-based pyrochlore phase during the beginning stages of sintering process, which reduces the electrical properties of the material, is a major obstacle observed in the fabrication of PMN-PT ceramics. Therefore, several studies

have been performed to eliminate the pyrochlore phase during synthesis. The various properties of PMN-PT ceramics based on different synthesis methods are listed in Table 1 [10–20]. As shown in Table 1, PMN-PT piezoelectric ceramics prepared by the partial oxalate method tend to show a higher piezoelectric charge coefficient (d_{33}) of 665 pC/N with a higher density of 8.23 g/cm^3. Among the several processing methods used to fabricate PMN-PT ceramics to form pure pervoskite phase, the Columbite precursor method has been widely used due to higher yield of perovskite phase content [21]. The Columbite precursor method can synthesize raw material corresponding to B-site in perovskite structure in ABO$_3$, prior to the reaction with lead. However, this Columbite method has demerits in the formation of pyrochlore phase during the sintering process. Also, several other fabrication methods such as sol-gel method, KCl molten salt method, and hot pressing have been performed and analyzed to improve piezoelectric properties by eliminating the pyrochlore phase. However, most of them leave a residual pyrochlore phase in the sintered ceramics [8,22,23].

Table 1. Comparison of various properties of $(1-x)$PMN-xPT ceramics based on different synthesis methods.

Method	d_{33} (pC/N)	k_p (%)	ρ (g/cm^3)	ε_r (1 kHz)	T_c (°C)	Ref.
Mixed oxide	430	56.4	7.85	2547	162	[10]
Mechanochemical	570	-	-	-	171	[11]
Columbite	610	-	-	6350	-	[12]
Columbite	499	52	-	4830	180	[13]
Columbite	530	-	7.8	-	153	[14]
Spark plasma sintering	350	57	-	-	-	[15]
Spark plasma sintering	590	63.4	-	-	160	[16]
Molten salts	660	-	-	-	165	[17]
Molten salts	540	66	7.73	-	144.5	[18]
Partial oxalate	590	57	7.828	2617.9 (100 Hz)		[19]
Partial oxalate	581	56.5	7.97	-	151	[20]
Partial oxalate	665	77.8	8.23	3230	129.84	Our sample

The partial oxalate method is an innovative technique to remove the pyrochlore phase of lead-based ceramics. This method has been successfully investigated for the synthesis of PZT, PLZT and PMN [24,25].

In this study, after making B-site compound of ABO$_3$ structure using columbite precursor method, MN and PT powders were coated with the needed amount of lead oxalate followed by calcination to form the PMN-PT. $(1-x)$PMN-xPT ceramics were prepared using a partial oxalate method to remove the pyrochlore phase at various sintering temperatures. The influence of synthesis method on the dielectric, piezoelectric, and ferroelectric properties of PMN-PT ceramics was investigated. Also, we have investigated $(1-x)$PMN-xPT ceramics, focusing on the effects of MPB region according with PT content with respect to using applications.

2. Materials and Methods

$(1-x)$PMN-xPT (x = 0.250, 0.300, 0.325, 0.350, 0.400 mol) ceramics were prepared using the partial oxalate method [26]. Reagent-grade MgO (Sigma Aldrich, Saint Louis, MI, USA, 99.0%), Nb$_2$O$_5$ (Sigma Aldrich, 99.9%), TiO$_2$ (Sigma Aldrich, 99.9%), Pb(NO$_3$)$_2$ (Sigma Aldrich, 99.0%), and oxalic acid (Sigma Aldrich, 99.0%) powders were used as starting materials. The weighed powders (MgO, Nb$_2$O$_5$) according to the stoichiometry of composition were mixed in high-purity ethanol (EMD Millipore, Burlington, MA, USA, 99.9%) for 6 h by planetary ball milling with a zirconia ball, then calcined at 1100 °C for 4 h. The stoichiometric MN and TiO$_2$ powders were mixed in high-purity ethanol for 6 h by planetary ball milling with zirconia balls, then calcined at 1100 °C for 4 h. The weight ratio between the balls and powders were 10:1. Until now, very rare papers were reported for the partial oxalate processing techniques for the PMN ceramics case. Also, there is no papers for the PMN-PT

piezoelectric ceramics with improved piezoelectric properties by comparing existence of pyrochlore phase. The partial oxalate process was carried out at 90 °C because this temperature enhances the reaction with oxalic acid to form soluble $Pb(MNT)OC_2O_4 \cdot H_2O$ species. The processing steps of the oxalic process may be described by the following equations:

$$(MNT)O_2 + H_2C_2O_4 + H_2O \rightarrow (MNT)OC_2O_4 + 2H_2O \tag{1}$$

$$(MNT)OC_2O_4 + Pb(NO_3)_2 + H_2C_2O_4 + H_2O \rightarrow Pb(MNT)OC_2O_4 \cdot H_2O_{(s)} + 2HNO_3 \tag{2}$$
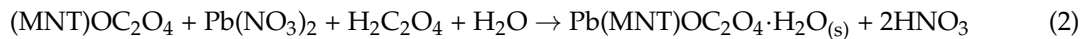
The coated $Pb(MNT)OC_2O_4 \cdot H_2O$ powders were washed several times, first with distilled water and then with high-purity ethanol, prior to being separated by filtration. The oxalate-coated $Pb(MNT)OC_2O_4 \cdot H_2O$ powders were dried at 120 °C, then calcined at 750 °C for 4 h. The $(1-x)$PMN-xPT powders were crushed and milled using high-purity ethanol as a ball milling for 12 h and calcined again at 750 °C for 4 h. The $(1-x)$PMN-xPT powders were pressed into a disc (12 mm diameter × 1.5 mm thickness) at a pressure of 294 MPa using polyvinyl alcohol (PVA) as a binder. After burning off the PVA (600 °C, 1 h) the pellets were sintered at 1200–1300 °C (1200, 1225, 1250, 1275 and 1300 °C) for 4 h.

The structures were examined by X-ray diffraction (XRD) analysis (New D8-Advance, Bruker-AXS, Billerica, MA, USA). The measurements were carried out from 20–70° by 0.02° differences. The wave-length of incident beam is around 1.54 Å from CuK_α radiation source. The microstructures of the ceramics were observed by field emission scanning electron microscopy (FE-SEM) (SIGMA, Carl Zeiss, Upper Cohen, Germany). The frequency-dependent and temperature-dependent dielectric constant (ε_r) of these ceramics were analyzed. Polarization versus electric (P-E) hysteresis loops and strain versus electric (S-E) loops of the ceramic were then measured. The piezoelectric charge coefficient (d_{33}) and planar electromechanical coupling factor (k_p) were measured by the Berlin-court quasi-static meter (YE2730A, APC International, Ltd., Mackeyville, PA, USA) and impedance analyzer (Agilent 4294A, Agilent Technologies, Santa Clara, CA, USA), respectively.

3. Results and Discussion

Figure 1 presents XRD patterns of 0.675PMN-0.325PT ceramics synthesized by the Columbite method and partial oxalate process sintered at 1275 °C. The PMN-PT ceramic prepared by the partial oxalate process was found to produce a pure perovskite phase, while the PMN-PT ceramic obtained by the Columbite method was found to produce a pyrochlore phase.
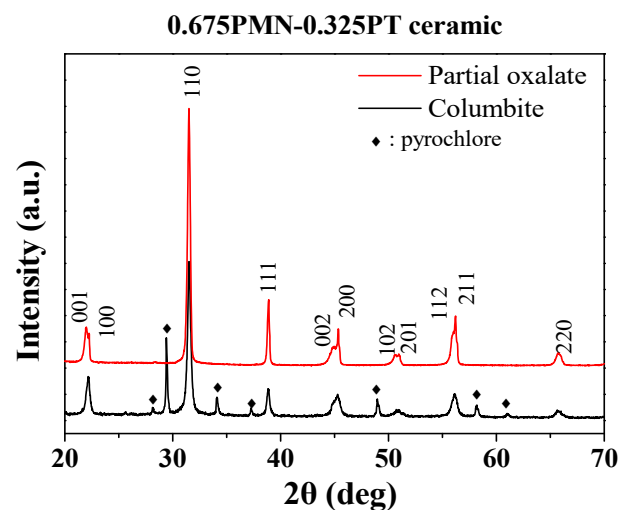
Figure 1. X-ray diffraction θ–2θ scans with CuK_α radiation of the 0.675PMN-0.325PT ceramics synthesized by Columbite method and partial oxalate process sintered at 1275 °C.

Figure 2a shows XRD patterns using a log-scale of the $(1-x)$PMN-xPT (x = 0.250, 0.300, 0.325, 0.350, 0.400 mol) ceramics sintered at 1275 °C. The XRD patterns were measured from 20 to 70° at 0.02° intervals for 0.5 h, respectively. Although the XRD figures were shown in the log scale in the Y -axis, any pyrochlore phase was not observed. As shown in the Figure 2a, a pure perovskite phase was observed for all specimens without any pyrochlore phase. This indicates that the partial oxalate method effectively removed the pyrochlore phase and assisted to form the PMN-PT ceramic. Figure 2b describes the Bragg reflection of the $(1-x)$PMN-xPT from 44 to 46°. A PT composition of 0.250 mol shows the rhombohedral phase. Then, as the PT composition increased up to 0.400 mol, the (200) peak positions moved to the higher angle, and confirmed (002)/(200) peak splitting at PT composition of 0.400 mol. This indicated that mixed rhombohedral and tetragonal phases (MPB region) are present between the PT composition from 0.325 to 0.350 mol. Also, that composition could show the highest piezoelectric, dielectric, and ferroelectric properties compared with other specimens.
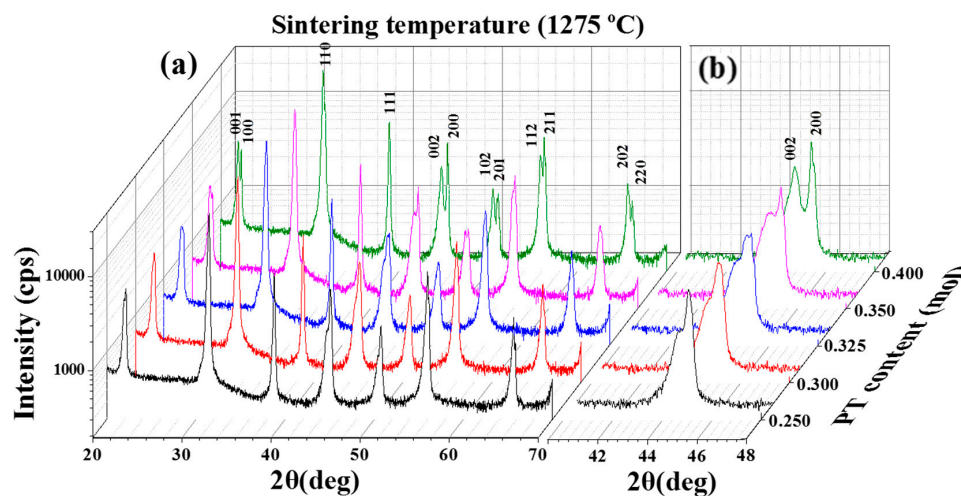
Figure 2. X-ray diffraction θ–2θ scans with CuK$_{\alpha}$ radiation for the $(1-x)$Pb(Mg$_{1/3}$Nb$_{2/3}$)O$_3$-xPbTiO$_3$ (x = 0.250, 0.300, 0.325, 0.350, 0.400 mol) ceramics sintered at 1275 °C (**a**) from 20 to 70 °and (**b**) from 40 to 48 °.

Figure 3 displays cross-sectional FE-SEM images of the $(1-x)$PMN-xPT (x = 0.250, 0.300, 0.325, 0.350, 0.400 mol) ceramics sintered at 1275 °C and the 0.650PMN-0.350PT ceramics depending on a sintering temperature from 1200 to 1300 °C. After polishing cross-sections of all specimens, they were thermally etched for 10 min at a temperature of 100 °C lower than the sintering temperature.
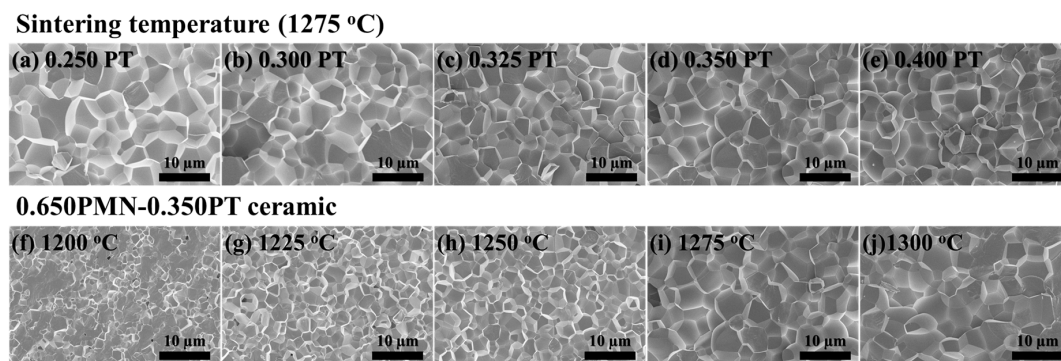
Figure 3. FE-SEM micrographs of the cross-sections after thermal etching; (**a**) 0.750Pb(Mg$_{1/3}$Nb$_{2/3}$)O$_3$-0.250PbTiO$_3$; (**b**) 0.700Pb(Mg$_{1/3}$Nb$_{2/3}$)O$_3$-0.300PbTiO$_3$; (**c**) 0.675Pb(Mg$_{1/3}$Nb$_{2/3}$)O$_3$-0.325PbTiO$_3$, (**d**) 0.650Pb(Mg$_{1/3}$Nb$_{2/3}$)O$_3$-0.350PbTiO$_3$, and (**e**) 0.600Pb(Mg$_{1/3}$Nb$_{2/3}$)O$_3$-0.400PbTiO$_3$, ceramics sintered at 1275 °C and the 0.650Pb(Mg$_{1/3}$Nb$_{2/3}$)O$_3$-0.350PbTiO$_3$ ceramics sintered at (**f**) 1200 °C, (**g**) 1225 °C, (**h**) 1250 °C, (**i**) 1275 °C, and (**j**) 1300 °C.

Platinum (Pt) coating using an ion-coater was carried out for 120 s, and all samples were measured under the same conditions at 7000 magnifications. 0.750PMN-0.250PT ceramics showed a relatively large grain size of approximately 6.75 µm compared with that of other composition ceramics. The increasing amount of PT substitution in the PMN composition can cause not only lattice distortion but also dwindle the grain size of these ceramics, as shown in the Figure 3a. Otherwise, when the sintering temperature increased up to 1300 °C, grain size was increased compared with 0.650PMN-0.350PT sintered at 1200 °C as shown in the Figure 3b. As increasing the sintering temperature, grain size increases because of stress relaxation. This result could be explained by the phenomenological kinetic grain growth equation [27,28].

Figure 4 illustrates the dielectric constants (ε_r) and dielectric losses of the $(1-x)$PMN-xPT (x = 0.250, 0.300, 0.325, 0.350, 0.400 mol) ceramics sintered at 1275 °C and the 0.650PMN-0.350PT ceramics sintered from 1200 to 1300 °C depending on the frequency range. The dielectric properties were measured from 1 kHz to 1 MHz. The ε_r was calculated from the computed capacitance by an impedance analyzer through the following equation:

$$\varepsilon_r = \frac{C \cdot d}{\varepsilon_0 \cdot A} \tag{3}$$

where C was the capacitance of the sample, d was the sample thickness, A was the area of the electrode, and ε_0 was the dielectric constant of a vacuum (8.854×10^{-14} F/cm). Based on the equation, the ε_r of PT composition of 0.350 mol is higher than that of other compositions, with a maximum value of 3230 at 1 kHz. Then, it decreases when PT composition is above 0.350 mol. This tendency is attributed to the occurrence of phase transition that was previously verified by analysis of XRD pattern as shown in Figure 2b.
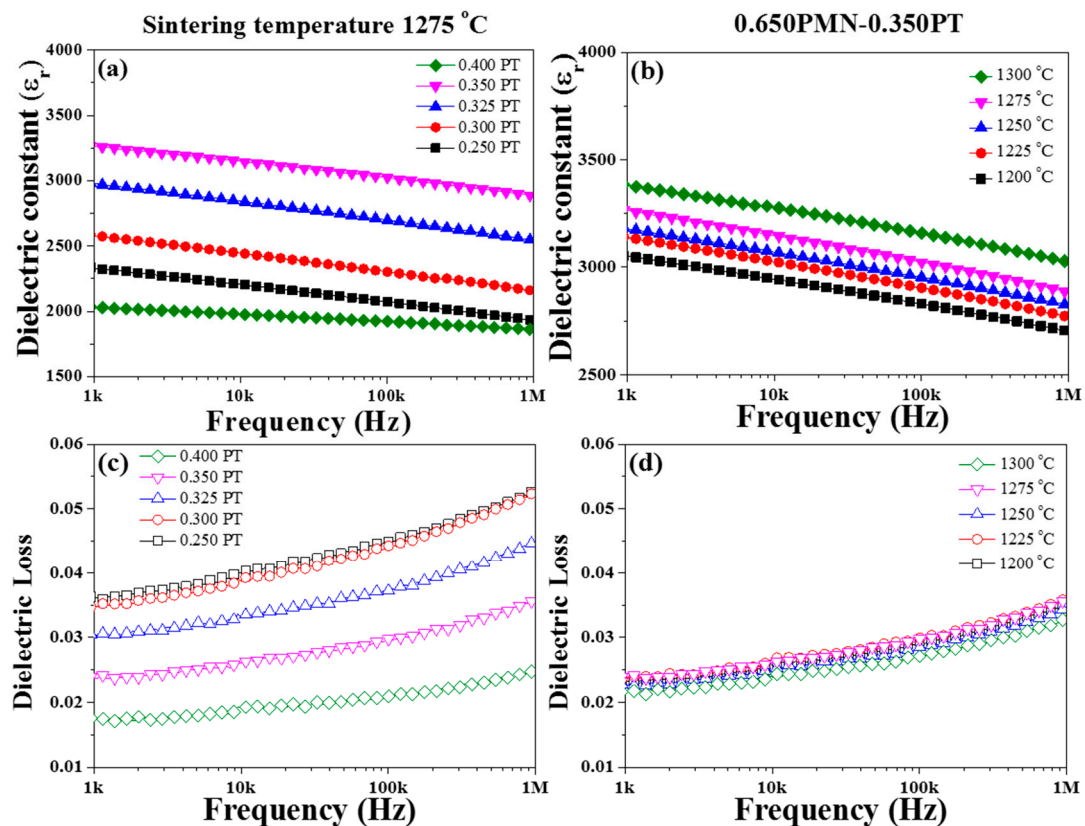
Figure 4. Frequency-dependent dielectric constant and dielectric losses; (**a**) dielectric constant and (**c**) dielectric losses the $(1-x)$Pb(Mg$_{1/3}$Nb$_{2/3}$)O$_3$-xPbTiO$_3$ (x = 0.250, 0.300, 0.325, 0.350, 0.400 mol) ceramics sintered at 1275 °C and (**b**) dielectric constant and (**d**) dielectric losses the 0.650Pb(Mg$_{1/3}$Nb$_{2/3}$)O$_3$-0.350PbTiO$_3$ ceramics sintered from 1200 to 1300 °C.

The dielectric losses of the (1−*x*)PMN-*x*PT (*x* = 0.250, 0.300, 0.325, 0.350, 0.400 mol) ceramics sintered at 1275 °C were decreased as increasing the PT composition, indicating that PT can usefully decrease dielectric loss. Additionally, we found that by increasing the sintering temperature up to 1300 °C, the ε_r value was increased by about 1.07 times at 1 kHz compared to that of 1200 °C as shown in the Figure 4b. The measured ε_r of 0.650PMN-0.350PT ceramic sintered at 1300 °C is around 3278 at 1 kHz. This result correlates to grain size and sintering temperature. As increasing the sintering temperature, grain size can cause not only a decrease of grain-boundary volume but also increase in the ε_r of 0.650PMN-0.350PT ceramic.

Figure 5a shows a piezoelectric charge coefficient (d_{33}) of the (1−*x*)PMN-*x*PT (*x* = 0.250, 0.300, 0.325, 0.350, 0.400 mol) ceramics sintered from 1200 to 1300 °C. The d_{33} increased with increasing PT composition up to 0.350 mol and sintering temperature up to 1275 °C, with a maximum d_{33} of 665 pC/N. Figure 5b displays planar electromechanical coupling factor (k_p) of the (1−*x*)PMN-*x*PT (*x* = 0.250, 0.300, 0.325, 0.350, 0.400 mol) ceramics sintered from 1200 to 1300 °C. These tendencies of k_p were like those of d_{33}. The k_p were calculated by using the following equation [29]:

$$k_p = \sqrt{2.529 \times \frac{(f_a^2 - f_r^2)}{f_r^2}} \tag{4}$$

where f_a and f_r are the anti-resonance and the resonance frequency, respectively. The maximum value of k_p was 77.8% in 0.650PMN-0.350PT at 1275 °C. As a result, these increased d_{33} and k_p were related with each composition and MPB region, as discussed in Figure 2b.
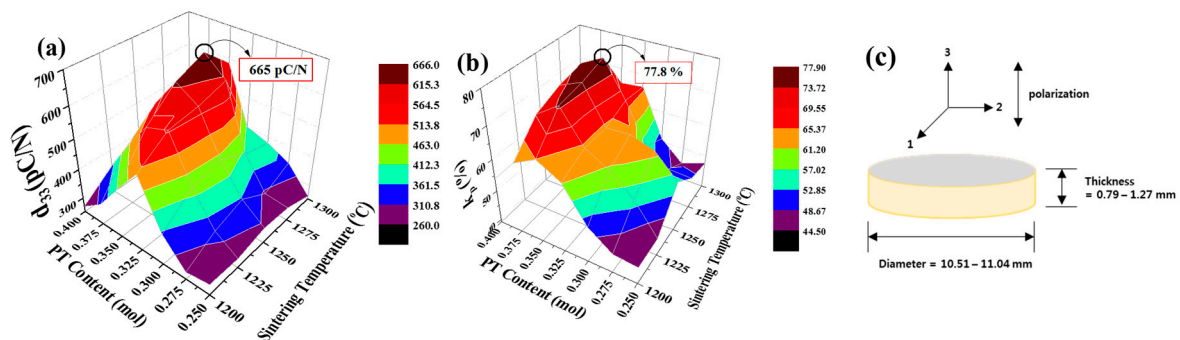
Figure 5. (**a**) piezoelectric charge coefficient (d_{33}), (**b**) planar electromechanical coupling factor (k_p), and (**c**) the graphic geometry used for the (1−*x*)Pb(Mg$_{1/3}$Nb$_{2/3}$)O$_3$-*x*PbTiO$_3$ (*x* = 0.250, 0.300, 0.325, 0.350, 0.400 mol) ceramics sintered from 1200 to 1300 °C.

Figure 6 illustrates the temperature-dependent dielectric constant (ε_r) at 1 kHz for the (1−*x*)PMN-*x*PT (*x* = 0.250, 0.300, 0.325, 0.350, 0.400 mol) ceramics sintered at 1275 °C. The (1−*x*)PMN-*x*PT ceramic samples showed a temperature of maximum dielectric constant (T_m) of 84.12, 102.33, 115.59, 129.84, and 150.07 °C for PT composition of 0.250, 0.300, 0.325, 0.350, 0.400 mol, respectively. As shown in Figure 6, the T_m increased with increasing contents of PT up to 0.400 mol, reaching a maximum value of 150.07 °C, because PT has a Curie temperature of 490 °C. Also, PMN-PT ceramics show ferroelectric properties at temperatures above T_m unlike normal ferroelectric materials because of relaxor property.
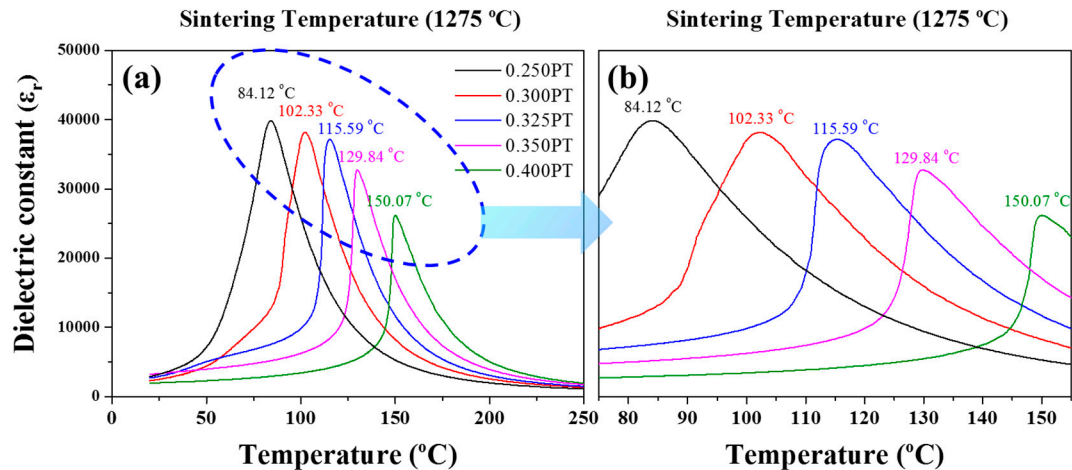
Figure 6. Temperature-dependent dielectric constant (ε_r) at 1 kHz for the $(1-x)$Pb($Mg_{1/3}Nb_{2/3}$)O_3-xPbTiO$_3$ (x = 0.250, 0.300, 0.325, 0.350, 0.400 mol) ceramics sintered at 1275 °C. (**a**) Dielectric constant (ε_r) from 25 °C to 250 °C; (**b**) dielectric constant (ε_r) from 75 °C to 155 °C.

Figure 7 shows P-E hysteresis loop for the $(1-x)$PMN-xPT (x = 0.250, 0.300, 0.325, 0.350, 0.400 mol) ceramics sintered at 1275 °C. The P-E hysteresis loops were measured by a Sawyer–Tower circuit under an applied electric field of 20 kV/cm at 0.1 Hz. With an increasing PT composition, the coercive electric field (E_c) was decreased. Whereas saturation polarization (P_s) and remnant polarization (P_r) increased up to 39.42 μC/cm^2 and 31.67 μC/cm^2, respectively, and the P-E loop revealed the presence of a typical hysteresis loop of ferroelectric materials. Also, 0.600PMN-0.400PT ceramics showed large E_c which is attributed to smaller grain size (Figure 3). It is well known that as grain size decrease, grain boundary area increases and most of the field is lost. Additionally, because of built-in bias fields, accumulation of space charge and unbalances of electrodes, the P-E loops show discontinuity [30,31].
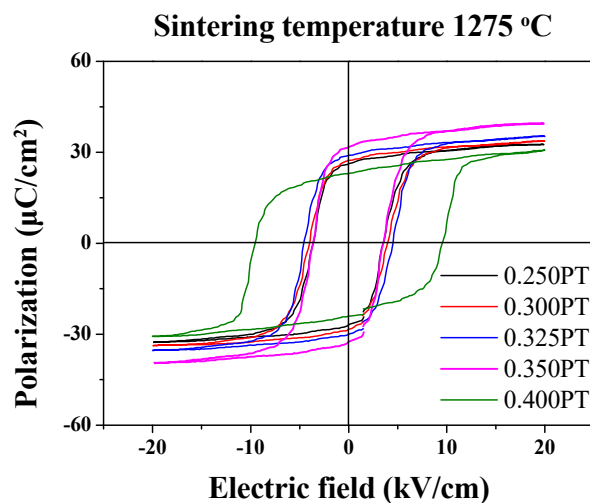
Figure 7. P-E hysteresis loop for the $(1-x)$Pb($Mg_{1/3}Nb_{2/3}$)O_3-xPbTiO$_3$ (x = 0.250, 0.300, 0.325, 0.350, 0.400 mol) ceramics sintered at 1275 °C.

Figure 8 shows bipolar S-E loop for the $(1-x)$PMN-xPT (x = 0.250, 0.300, 0.325, 0.350, 400 mol) ceramics sintered at 1275 °C. The strain increased up to a PT composition of 0.350 mol and the maximum value of strain was 0.12%. However, upon further increasing the PT composition, the strain began to decrease. Negative strain behavior of all specimens was observed. This result agreed well with the previous data for ε_r, d_{33}, k_p of $(1-x)$PMN-xPT ceramics sintered at 1275 °C.

Sintering temperature (1275 ºC)
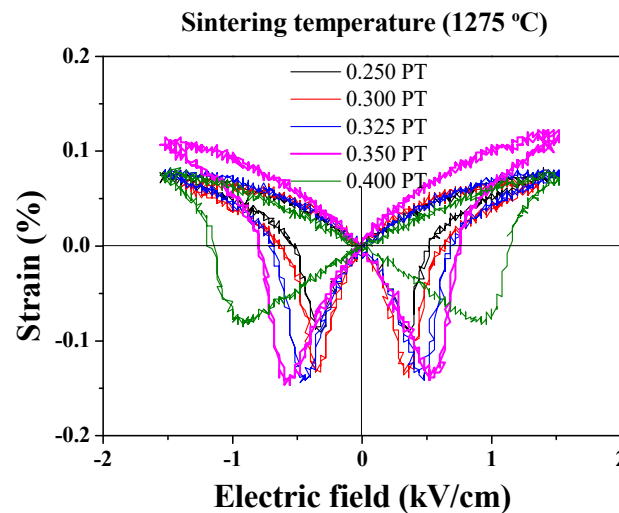
Figure 8. Bipolar S-E loop for the $(1-x)Pb(Mg_{1/3}Nb_{2/3})O_3-xPbTiO_3$ (x = 0.250, 0.300, 0.325, 0.350, 400 mol) ceramics sintered at 1275 °C.

Figure 9 shows a P-E hysteresis loop for the 0.650PMN-0.350PT ceramic from 40 to 170 °C. In all P-E loop data, the observed P_r and E_c decreased as the temperature increased and showed a ferroelectric property at temperatures above T_m, as discussed in Figure 6. The P-E hysteresis loop measured from 40 to 150 °C showed typical ferroelectric behavior. However, the P-E hysteresis loops changed at 170 °C, exhibiting paraelectric properties, meaning that an increased temperature caused phase transition from ferroelectric to paraelectric phase.

Sintering temperature 1275 ºC
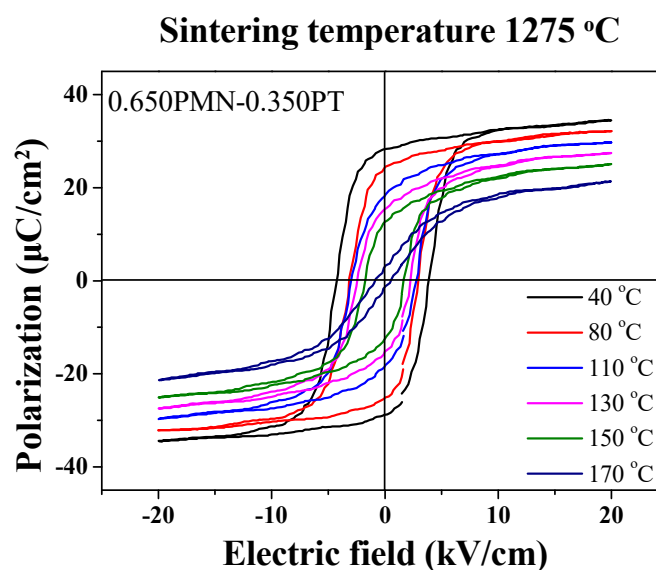
Figure 9. Temperature-dependent P-E hysteresis loop for the $0.650Pb(Mg_{1/3}Nb_{2/3})O_3-0.350PbTiO_3$ ceramic sintered at 1275 °C.

4. Conclusions

The $(1-x)$PMN-xPT ceramics with outstanding piezoelectric and ferroelectric properties have been investigated and analyzed based on a partial oxalate process. As mentioned in XRD patterns, all specimens showed pure pervoskite structure without the pyrochlore phase. At the 0.325 and 0.350 mol of PT near the MPB region between the rhombohedral-tetragonal phase, higher piezoelectric properties were observed. We observed the maximum value of the d_{33} of 665pC/N and k_p of 77.8% from the 0.650PMN-0.350PT ceramic sintered at 1275 °C. The relaxor ferroelectric property of $(1-x)$PMN-xPT ceramics was confirmed through temperature-dependent ε_r and P-E loop. Therefore, these outstanding

properties suggest that 0.650PMN-0.350PT ceramics sintered at 1275 °C could be suitable for various applications substitutes for PZT as the relaxor ferroelectric material.

References

1. Swartz, S.L.; Shrout, T.R.; Schulze, W.A.; Cross, L.E. Dielectric Properties of Lead-Magnesium Niobate Ceramics. *J. Am. Ceram. Soc.* **1984**, *67*, 311–315. [CrossRef]

2. Papet, P.; Dougherty, J.P.; Shrout, T.R. Particle and grain size effects on the dielectric behavior of the relaxor ferroelectric Pb(Mg$_{1/3}$Nb$_{2/3}$)O$_3$. *J. Mater. Res.* **1990**, *5*, 2902–2909. [CrossRef]

3. Chaudhari, V.A.; Bichile, G.K. Systhesis, Structural, and Electrical Properties of Pure PbTiO$_3$ Ferreelectric Ceramics. *Smart Mater. Res.* **2013**, *132*, 1031–1038. [CrossRef]

4. Huang, H.; An, Z.; Huang, P.; Li, D.; Liao, Q. Phase transition and thermal depolarization of double perovskite modified low sintering temperature PbTiO$_3$ piezoelectric ceramics. *J. Eur. Ceram. Soc.* **2016**, *36*, 925–929. [CrossRef]

5. Slodczyk, A.; Colomban, P. Probing the Nanodomain Origin and Phase Transition Mechanisms in (Un)Poled PMN-PT Single Crystals and Textured Ceramics. *Materials* **2010**, *3*, 5007–5028. [CrossRef] [PubMed]

6. Pullano, S.A.; Mahbub, I.; Islam, S.K.; Fiorillo, A.S. PVDF Sensor Stimulated by Infrared Radiation for Temperature Monitoring in Microfluidic Devices. *Sensors* **2017**, *17*, 850. [CrossRef] [PubMed]

7. Xia, Z.; Wang, L.; Yan, W.; Li, Q.; Zhang, Y. Comparative investigation of structure and dielectric properties of Pb(Mg$_{1/3}$Nb$_{2/3}$)O$_3$-PbTiO$_3$ (65/35) and 10% PbZrO$_3$-doped Pb(Mg$_{1/3}$Nb$_{2/3}$)O$_3$-PbTiO$_3$ (65/35) ceramics prepared by a modified precursor method. *Mater. Res. Bull.* **2007**, *42*, 1715–1722. [CrossRef]

8. Leite, E.R.; Scotch, A.M.; Khan, A.; Li, T.; Chan, H.M.; Harmer, M.P.; Liu, S.F.; Park, S.E. Chemical Heterogeneity in PMN-35PT Ceramics and Effects on Dielectric and Piezoelectric Properties. *J. Am. Ceram. Soc.* **2002**, *85*, 3018–3024. [CrossRef]

9. Choi, S.W.; Shrout, T.R.; Jang, S.J.; Bhalla, A.S. Morphotropic Phase Boundary in Pb(Mg$_{1/3}$Nb$_{2/3}$)O$_3$-PbTiO$_3$ system. *Mater. Lett.* **1989**, *8*, 253–255. [CrossRef]

10. Zhong, N.; Dong, X.L.; Sun, D.Z.; Xiang, P.H.; Du, H. Electrical properties of Pb(Mg$_{1/3}$Nb$_{2/3}$)O$_3$-PbTiO$_3$ ceramics modified with WO$_3$. *Mater. Res. Bull.* **2004**, *39*, 175–184. [CrossRef]

11. Alguero, M.; Alemany, C.; Jimenez, B.; Holc, J.; Kosec, M.; Pardo, L. Piezoelectric PMN-PT ceramics from mechanochemically activated precursors. *J. Eur. Ceram. Soc.* **2004**, *247*, 937–940. [CrossRef]

12. Koo, T.Y.; Cheong, S.W. Dielectric and piezoelectric enhancement due to 90° domain rotation in the tetragonal phase of Pb(Mg$_{1/3}$Nb$_{2/3}$)O$_3$-PbTiO$_3$. *Appl. Phys. Lett.* **2002**, *80*, 4205–4207. [CrossRef]

13. Pham-Thi, M.; Augier, C.; Dammak, H.; Gaucher, P. Fine grains ceramics of PIN-PT, PIN-PMN-PT and PMN-PT systems: Drift of the dielectric constant under high electric field. *Ultrasonics* **2006**, *44*, e627–e631. [CrossRef] [PubMed]

14. Kumar, P.; Singh, S.; Thakur, O.P.; Prakash, C.; Goel, T.C. Study of lead Magnesium Niobate-Lead Titanate Ceramics for Piezo-Actuator Applications. *Jpn. J. Appl. Phys.* **2004**, *43*, 1501–1506. [CrossRef]

15. Zuo, R.; Granzow, T.; Lupascu, D.C.; Rodel, J. PMN-PT Ceramics Prepared By Spark Plasma Sintering. *J. Am. Ceram. Soc.* **2007**, *90*, 1101–1106. [CrossRef]

16. Park, J.K.; Chung, U.J.; Hwang, N.M.; Kim, D.Y. Preparation of Dense Lead Magnesium Niobate-Lead Titanate (Pb(Mg$_{1/3}$Nb$_{2/3}$)O$_3$-PbTiO$_3$) Ceramics by Spark Plasma Sintering. *J. Am. Ceram. Soc.* **2001**, *84*, 3057–3059. [CrossRef]

17. Zhao, S.; Li, Q.; Feng, Y.; Nan, C. Microstructure and dielectric properties of PMN-PT ceramics prepared by the molten salts method. *J. Phys. Chem. Solids* **2009**, *70*, 639–644. [CrossRef]

18. Xia, F.; Wang, X.; Zhang, L.; Yao, X. Dielectric and piezoelectric properties of PMN-PT ceramics prepared by molten salt synthesis. *Ferroelectrics* **1998**, *215*, 181–186. [CrossRef]

19. Fang, B.; Qian, K.; Chen, Z.; Yuan, N.; Ding, J.; Zhao, X.; Xu, H.; Luo, H. Large strain and pyroelectric properties of $Pb(Mg_{1/3}Nb_{2/3})O_3$-$PbTiO_3$ ceramics prepared by partial oxalate route. *Funct. Mater. Lett.* **2014**, *7*, 1450059. [CrossRef]

20. Qian, K.; Fang, B.; Du, Q.; Ding, J.; Zhao, X.; Luo, H. Phase development and electrical properties of $Pb(Mg_{1/3}Nb_{2/3})O_3$-$PbTiO_3$ ceramics prepared by partial oxalate route. *Phys. Status Solidi A* **2013**, *210*, 1149–1156. [CrossRef]

21. Kelly, J.; Leonard, M.; Tantigate, C.; Safari, A. Effect of Composition on the Electromechanical Properties of $(1-x)Pb(Mg_{1/3}Nb_{2/3})O_3$-$xPbTiO_3$ Ceramics. *J. Am. Ceram. Soc.* **1997**, *80*, 957–964. [CrossRef]

22. Ravindranathan, P.; Komarneni, S.; Bhalla, A.S.; Roy, R. Systhesis and Dielectric Properties of Solution Sol-Gel-Derived $0.9Pb(Mg_{1/3}Nb_{2/3})O_3$-$0.1PbTiO_3$ Ceramics. *J. Am. Ceram. Soc.* **1991**, *74*, 2996–2999. [CrossRef]

23. Katayama, K.; Abe, M.; Akiba, T. Sintering and Dielectric Properties of Single-Phase $Pb(Mg_{1/3}Nb_{2/3})$ O_3-$PbTiO_3$. *J. Eur. Ceram. Soc.* **1989**, *5*, 183–191. [CrossRef]

24. Gupta, S.M.; Kulkarmi, A.R. Synthesis of perovskite lead magnesium niobate using partial oxalate method. *Mater. Res. Bull.* **1993**, *28*, 1295–1301. [CrossRef]

25. Mergen, A.; Lee, W.E. Fabrication, Characterisation and Formation Mechanim of $Ph1.83Mg0.29Nb1.17O6.39$ Phrochlore. *J. Eur. Ceram. Soc.* **1997**, *17*, 1033–1047. [CrossRef]

26. Jayasingh, E.M.; Prabhakaran, K.; Sooraj, R.; Durgaprasad, C.; Sharma, S.C. Syntheis of pyrochlore free PMN-PT powder by partial oxalate process route. *Ceram. Int.* **2009**, *35*, 591–596. [CrossRef]

27. Chang, L.M.; Hou, Y.D.; Zhu, M.K.; Yan, H. Effect of sintering temperature on the phase transition and dielectrical response in the relaxor-ferroelectric-system 0.5PZN-0.5PZT. *J. Appl. Phys.* **2007**, *101*, 034101. [CrossRef]

28. Chen, T.Y.; Chu, S.Y.; Juang, Y.D. Effects of sintering temperature on the dielectric and piezoelectric properties of Sr additive Sm-modified $PbTiO_3$ ceramics. *Sens. Actuators A* **2002**, *102*, 6–10. [CrossRef]

29. Kwon, Y.H.; Shin, D.J.; Lee, G.H.; Koh, J.H. Sintering temperature dependent piezoelectric properties of $(Bi,Na)TiO_3$-$(Ba,Sr)TiO_3$ ceramics. *Ceram. Int.* **2016**, *42*, 10422–10427. [CrossRef]

30. Park, H.H.; Yoon, S.; Park, H.H.; Hill, R.H. Electrical properties of PZT thin films by photochemical deposition. *Thin Solid Films* **2004**, *447–448*, 669–673. [CrossRef]

31. Singh, R.; Chandra, S.; Sharma, S.; Tripathi, A.K.; Goel, T.C. Sol-Gel Derived La Modified PZT Thin Films: Structure and Properties. *IEEE Trans. Dielect. Electr. Insul.* **2004**, *11*, 264–270. [CrossRef]